Lithuanian Journal of Physics, Vol. **47**, No. 2, pp. 221–228 (2007) doi:10.3952/lithjphys.47206

CLEANING OF CONTAMINATED PAPER WITH THE SUBNANOSECOND Nd : YAG LASER PULSES

V. Švedas, A.S. Dement'ev, E. Murauskas, and N. Slavinskis

Laboratory of Nonlinear Optics and Spectroscopy, Institute of Physics, Savanorių 231, LT-02300 Vilnius, Lithuania
E-mail: svedas@ktl.mii.lt

Received 20 April 2007; revised 18 May 2007

Laser cleaning and restoration of documents on the paper base offer advantages over traditional mechanical and chemical cleaning methods. In this work, the office-type paper artificially contaminated for research purposes was cleaned with subnanosecond laser pulses. Laser cleaning recovered more than 80% of the paper initial brightness observed in the visible range, whereas chemical modifications of the paper studied by the FTIR spectrometer were below the spectrometric noise level. The laser fluences above the optical breakdown threshold of the paper surface resulted in the uplift of the paper surface and thinning-out of cellulose fibres in the breakdown zone. This type of morphological modification is accompanied by the FTIR detected compositional changes of the substrate – the intensity of three $CaCO_3$ infrared peaks decreases after laser treatment.

Keywords: paper, laser cleaning, Fourier Transform Infrared (FTIR) spectroscopy, photoacoustic spectroscopy

PACS: 82.80.Gk, 82.80.Kq

1. Introduction

Paper known to everybody as a carrier of written information contains interesting physics [1]. From the restoration point of view, cleaning of the historical paper documents presents a labour consuming task due to delicate substrate material. Usually the paper surface is first cleaned by mechanical methods and tools such as erasers or scalpels, and then it is chemically treated with water and chemical solvents. The paper surface damage or irreversible changes of the substrate structure and the chemical composition often result from the sequence of these ordinary cleaning procedures. The use of pulsed laser radiation for cleaning and restoration of historical documents and artworks has recently been proposed [2–9]. This technique allows avoiding negative effects found when using mechanical and chemical procedures to remove paper impurities. Moreover, the laser assures a non-contact well localized action, and also the computer control of the process.

The contamination matter is removed with the laser when the light fluence value exceeds some threshold values, which are different for different contamination types and contamination removal mechanisms. Cleaning can proceed by thermal shocking of the contamination particles or contamination crust [10, 11]. Heating of the contaminant above the evaporation temperature is not necessary in that case. Particles undergo thermal expansion on the nanoseconds temporal scale. At the particle-substrate contact point, ultra fast contaminant particle expansion gives rise to huge particle pressure towards the substrate. The pressure force is counterbalanced by the reaction force of the substrate which accelerates the contaminant particles and breaks them away from the substrate. The other method of cleaning applies pulse-by-pulse laser evaporation of contaminant. The evaporation threshold fluence can be evaluated using the known thermo-physical and optical parameters of contaminant [2].

Paper and other objects of cultural heritage are analysed and diagnosed by the non-invasive techniques [12, 13], infrared (IR) spectral analysis being among them [12–17]. For the purpose of laser cleaning process modelling and investigation, the paper sample is artificially contaminated with the iron salt solution [12] or black carbon [7, 9]. The majority of works regarding cleaning are conducted using about 5 to 10 ns laser pulses. The cleaning fluences are in the range from a bit smaller than 1 to a few $\mathrm{J/cm^2}$. The aim of this work was to process the artificially contaminated paper by the short 0.15 ns pulse Nd : YAG laser radiation and to investigate laser caused modifications of the paper substrate by three Fourier Transform Infrared (FTIR) spec-

ISSN 1648-8504

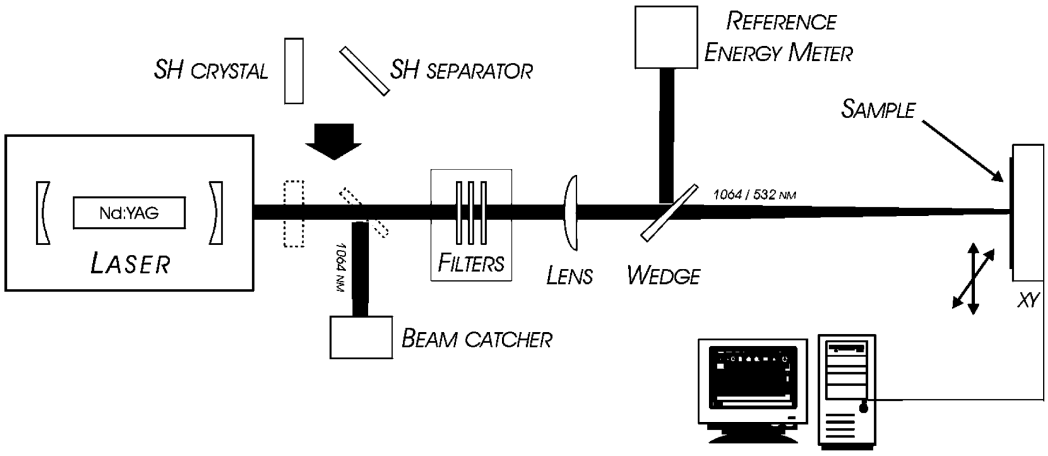

Fig. 1. Experimental set-up.

tra sampling methods: reflectance, transmittance, and photoacoustic detection.

2. Experimental

2.1. Apparatus and sample treatment

Paper was processed by Nd : YAG laser radiation. The actively Q-switched Nd : YAG laser [18] with pulse compression by stimulated Brillouin scattering [19] generates the 0.15 ns duration radiation pulse in the TEM_{00} mode, which is applied to the sample. A scheme of experimental set-up is shown in Fig. 1. Both the fundamental and second harmonics were used for paper processing. Unfocused radiation was employed for soft cleaning mode. In the hard radiation mode, radiation was focused by lens. The sample was placed out of the beam waist, i. e., radiation was only "pre-focused" on the sample to reach the optical breakdown threshold. Transversal beam dimensions at the sample holder place were controlled by the knife-edge method for fundamental harmonic and with the CCD camera in the case of the second harmonic.

Samples were prepared employing two kinds of the office A4 size paper: Data Copy and Mondi Business, futher referred to as DC and MB, respectively. Appropriate paper pieces were contaminated by dense painting of the surface by thick coal chalk lines. The area of the contaminated paper sufficient for the spectral analysis was cleaned. The low-intensity unfocused laser pulses were used for cleaning. Energy densities were below the evaporation threshold in that case. Samples were also treated with the focused laser pulse. In this case, for treating areas sufficient for FTIR analysis, the paper was placed on the computer driven X–Y moving stage.

FTIR spectra were measured with the Nicolet 8700 spectrometer in reflection and transmission modes. Reflection was measured with the FT30 accessory. Both the spectrometer and reflectance acccessory were from Thermo Electron Corporation, Madison WI, USA. Photoacoustic (PA) spectra of the paper were measured with the PAC-300 accessory (MTEC Photoacoustics, Inc., Ames IA, USA) which was mounted in the sample compartment of the FTIR spectrometer. The spectrometer operating in reflectance and transmittance modes can handle samples up to a few cm in width. In the PA spectroscopy, a piece of the sample is placed into the gas-tight sample holder head. Paper samples were fitted to the smallest 0.5 cm diameter sampling cup of the PAC-300 accessory. For this purpose, a suitable circle was cut with scissors.

2.2. FTIR photoacoustic spectroscopy

The desired result of spectral analysis is to obtain an analytical information with minimal or no sample preparation. However, spectral analysis of unprepared samples by the conventional transmittance and reflectance methods is often impractical because the sample can be optically too thick for transmittance measurements or it lacks the sufficient reflected flux for reflectance spectroscopy. Photoacoustic spectroscopy [14, 15] has the capabilities of direct infrared absorption method which employs the detection of sample heating by absorbed radiation.

For the PA analysis a piece of the sample is exposed to IR radiation in the air-tight chamber filled with helium or nitrogen. Heat generated within the sample due to the absorption of IR radiation transfers to the sample surface by heat diffusion. Due to the sample surface–gas heat exchange the chamber gas tempera-

ture increases that gives rise to the isochoric pressure increase in the chamber. Registered with the microphone this pressure increase is known as a photoacoustic signal. The photoacoustic signal contains information on the sample absorption coefficient and on the depth below the sample surface from which the signal evolves.

The FTIR interferometer modulates the intensity of the incident infrared beam, which due to the absorption decays exponentially deep down the sample. Absorbed radiation is converted into heat, causing the temperature of each absorbing infinitesimal layer to oscillate at the beam modulation frequency with the amplitude proportional to the amount of the absorbed light [20, 21]. Layers become a source generating propagating temperature oscillations or thermal waves. Thermal waves have important property affecting the acoustic wave generation. Thermal waves decay to the $1/\mathrm{e}$ level of their original amplitude over the distance L called the thermal decay length or thermal diffusion depth. L is given by the following equation [14]:

$$L = \left(\frac{D}{\pi f}\right)^{0.5}, \qquad (1)$$

where D and f denote the sample thermal diffusivity and the infrared beam modulation frequency, respectively.

The thermal decay length determines the PA sampling depth. The latter can be changed by varying the IR beam modulation frequency. The lower modulation frequency allows a longer time for thermal waves to propagate from deeper layers within the sample into the gas, thus allowing a larger sampling depth. For organic polymeric materials, D is of the order of 10^{-3} cm^2 s. Modulation frequency f is a product of the moving mirror optical path difference (OPD) velocity and the wave number. For the IR spectrum (350–7400 cm^{-1}), the values of f at the mirror OPD velocity value of the order of 0.1 cm/s are in the range of tens to hundreds Hz. According to Eq. (1) the respective sampling depth is of the order of a few to tens of micrometers.

The photoacoustic signal generation can be modelled using the heat equation and assuming a one-dimensional heat flow within the sample [14–15, 20, 21]. Within the sample the incident infrared beam decays exponentially with the sample absorption coefficient k. The PA signal dependence on the value of k is linear with the exception of extremes of low and high values of k. At very low values of k, some background signal, which does not depend on sample absorption, exceeds the PA sample signal. At high values of k, denoted by k_o, the signal experiences an onset of signal saturation and starts to loose sensitivity to increasing values of k. Complete saturation occurs at a higher value of k, denoted by k_s. For $k > k_\mathrm{s}$, the signal no longer senses increases in the absorption coefficient. Connections between the sample absorption properties and the thermal diffusion depth can be approximated by the rule of thumb values for k_o and k_s as a function of L [14]:

$$k_\mathrm{o} \cong \frac{1}{10\,L},$$

$$k_\mathrm{s} \cong \frac{20}{L}.$$

To correct the saturation effect of the PA signal, the linearization procedure is developed [14]. Both magnitude and phase of the PA signal are included into linearization. Properly linearized PA spectra vary linearly with k to approximately $100/L$ [14], that is, by three orders of magnitude above the onset of saturation. PA spectra measured at different modulation frequencies are commonly used for qualitative and quantitative analysis of samples having compositional variations as a function of depth.

3. Results and discussion

3.1. Reflectance and transmittance spectroscopy

Unfocused laser radiation was attenuated by the set of neutral density filters. To exceed the cleaning threshold, the pulse energy was increased by substituting filters with smaller transmittance by filters with larger transmittance until the cleaning started. When the cleaning threshold was exceeded, laser pulses produced the ∼3 mm spot visually free from carbon contaminant. The carbon contaminated DC paper was soft cleaned with the 1064 nm wavelength pulses of the 0.15 J/cm^2 energy density. This energy density value is almost by an order smaller than that needed for usual cleaning with nanosecond pulses.

Exposition of the spot of the paper to approximately ten to twenty pulses leads to satisfactory cleaning. Results of artificial contamination and laser cleaning were recorded with the Canon PowerShot S3 IS digital camera. Digital brightness of suitable areas of the sample was read on the $0, \ldots, 255$ scale by the cross-hair marker of imaging software. Brightness of the paper surface was estimated as follows. For contaminated areas it was in the 15 to 25 range as compared to the 238 to 241 brightness of the untreated paper. Brightness of the cleaned paper was approximately in the 195 to 205

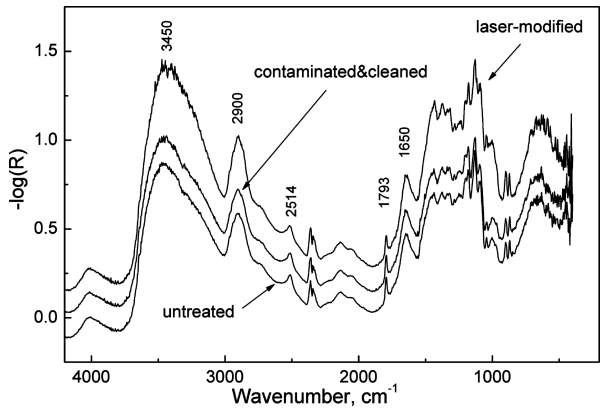

Fig. 2. Reflectance spectra of differently treated "Data Copy" office-type paper. Reflectances of untreated paper, contaminated and soft-cleaned, and laser-modified paper are shown. The resolution is 4 cm^{-1}. Offset of spectra is made for clarity.

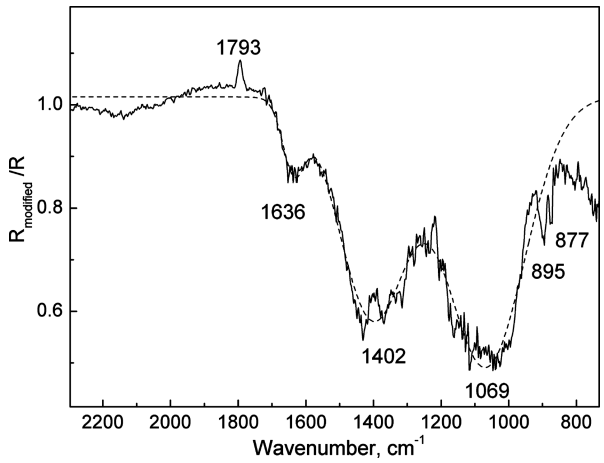

Fig. 3. Ratio spectrum of reflectances of laser-modified and untreated paper.

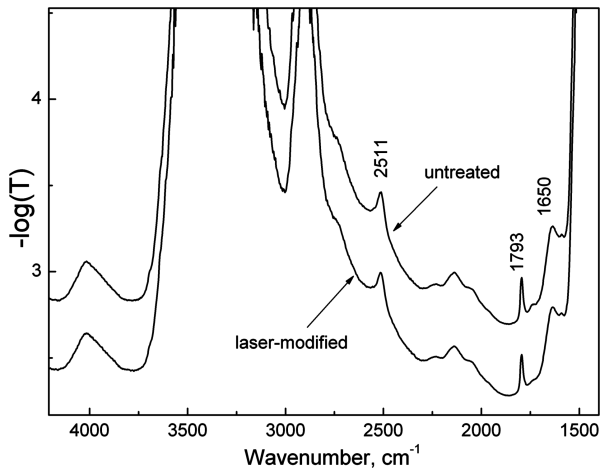

Fig. 4. Transmittance spectra of untreated and laser-modified "Mondi Business" office-type paper: The resolution is 4 cm^{-1}. Offset of spectra is made for clarity.

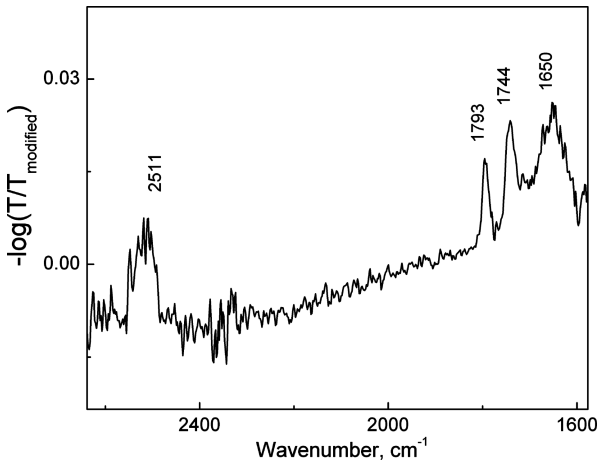

Fig. 5. Difference of laser-modified and untreated paper spectra.

range. Thus, soft laser cleaning recovers approximately 80% of the initial paper brightness.

In the hard treatment mode, the 10 mJ energy and the 1064 nm wavelength laser pulses were focused on the sample surface. Ten pulses were applied to each treatment spot. The area sufficient for FTIR sampling was created by the computer controlled sample X–Y translation. Hard treatment led to the uplifting of the paper surface and thinning-out of cellulose fibres.

The 4200–400 cm^{-1} range reflectance spectra of the differently treated DC paper are shown in Fig. 2. Paper samples show the same spectral structures irrespective of the treatment mode. The O–H and C–H fundamental stretch vibrations form the 3450 cm^{-1} and 2900 cm^{-1} bands, respectively [22]. The 1793 cm^{-1} peak and 2514 cm^{-1} band are the structures of the paper additive that can be ascribed to $CaCO_3$ [23]. The 1650 cm^{-1} band implies frequencies of bending vibration of adsorbed water O–H bonds. FTIR spectra of the untreated paper and the soft cleaned paper are very similar. No detectable variation in the shape of bands and peaks was found. Only spectrally featureless decrease of reflectance was observed. Spectral reflectance difference between the soft cleaned and untreated paper shows a decrease from 25 to 12% as the wave number decreases from 6000 to 1000 cm^{-1}. Evidently, spectrally featureless difference absorption is caused by the coal residuals.

The ratio spectrum in Fig. 3 shows the paper spectral variations after modification by the hard laser treatment. The ratio reveals the broad 1636, 1402, and 1069 cm^{-1} bands and the 1793 cm^{-1} peak. The 1793 cm^{-1} peak indicates the presence of calcium carbonate in the office-type paper. A positive sign of this peak in the ratio spectrum means an absorption decrease. Evidently, the absorption decrease shows that the amount

of $CaCO_3$ in the paper is diminished by laser treatment. Bands of the ratio spectrum are composed by vibrations of various bonds. Adsorbed water O–H contributes to the 1636 cm^{-1} band. The CH_3 methyl and CH_2 methylene C–H bond bending vibrations [22] contribute to the absorption of the 1402 cm^{-1} band. The cellulose macromolecule C–O–C stretches [22] both in the skeleton and glucopyranose ring site make up the 1069 cm^{-1} band. The 874 and 898 cm^{-1} peaks are "fingerprints" of $CaCO_3$ [23] and cellulose matrix molecules, respectively.

Investigating all relevant reasons for spectral differences of Figs. 2 and 3 one should separate spectral variations caused by chemical composition changes and variations of optical-physical properties. Among physical reasons that cause spectral differences, the thinning-out of cellulose fibres after laser hard treatment has the largest influence on the spectral magnitude. Due to the decrease of the cellulose packing density, the specific scattering coefficient of the paper decreases. The specific scattering coefficient is one of the parameters responsible for radiation transfer in the discontinuous materials such as paper and for the value of their diffuse reflection coefficient [24]. After hard laser treatment, increase in the 1636, 1402, and 1069 cm^{-1} band absorption is observed as shown in Fig. 3. Probably this absorption increase is caused by mentioned physical changes in the sample, i. e., thinning-out of fibres and decrease of the specific scattering coefficient.

The MB paper was hard treated with the 532 nm wavelength laser pulses of the 4 J/cm^2 fluence. In this treatment mode the 18 mJ energy laser pulse was focused on the sample surface to the 0.07×0.08 cm^2 ellipse spot. The area suitable for FTIR spectroscopy was created by the sample computer controlled movement in the X–Y direction in 0.05 cm steps. Three pulses were applied to each treatment spot. Thus the 1 cm^2 treated area was created by the scanned laser treatment. Transmittance spectra in absorbance units of the untreated and treated paper in the 4200–1500 cm^{-1} range are shown in Fig. 4. Absorbances in the 3500–2800 cm^{-1} range and in the range below 1500 cm^{-1} exceed 4.5. This absorbance value is too large to be measured with the used instrument. Noise in the mentioned spectral ranges fully masks any spectral features.

Transmittance spectra show the same features as reflectance spectra in Fig. 2. These are the 2511 and 1793 cm^{-1} peaks of $CaCO_3$ [23] and the 1650 cm^{-1} band of adsorbed water. Like reflectance spectra, transmittance spectra are affected by the radiation scattering that contributes to the resulting spectra both additively and multiplicatively [25, 26]. The contribution of scattering to transmittance spectra is mitigated by the multiplicative signal correction (MSC) procedure [25, 26]. For the sake of scattering correction, the MSC method was applied to the transmission spectrum of the treated paper. The difference spectrum of transmittance of the untreated and treated paper corrected by MSC is shown in Fig. 5. The same peaks as in Fig. 4 are observed in the difference spectrum. A positive sign of the 2511 and 1793 cm^{-1} peaks indicates the $CaCO_3$ absorption decrease that is evidently caused by the $CaCO_3$ concentration decrease caused by the laser treatment. The difference spectrum in Fig. 5 revealed the 1744 cm^{-1} peak, which probably indicates the presence of organic binder in the MB paper.

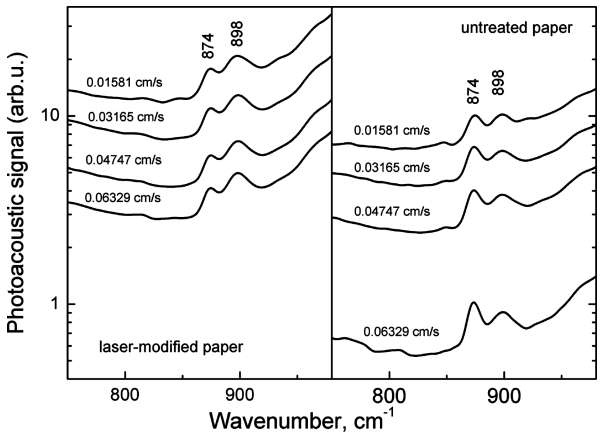

Fig. 6. Photoacoustic spectra of laser-modified and untreated paper as OPD velocity varies in steps from 0.01581 to 0.06329 cm/s. Spectral resolution is 8 cm^{-1}.

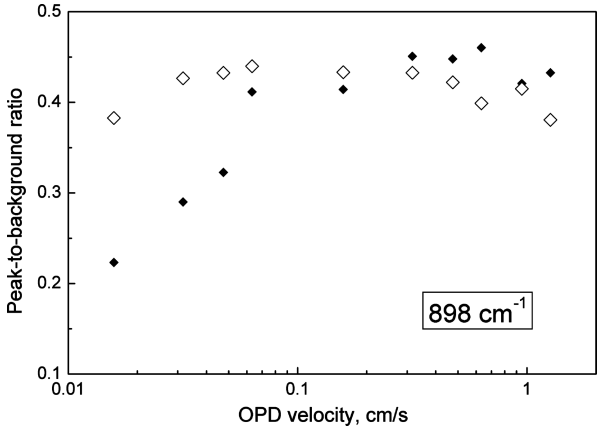

Fig. 7. The cellulose 898 cm^{-1} peak-to-background ratio versus OPD velocity for untreated paper (solid diamonds) and laser-modified paper (hollow diamonds).

3.2. Photoacoustic spectroscopy of laser treated and untreated paper

During measurement of PA spectra, the OPD velocity V of the moving spectrometer mirror was varied in steps from 0.01581 to 1.27 cm/s. The modulation frequency f of radiation was varied in the 0.01581ν to 1.27ν Hz range (here ν is the wave number in cm^{-1}). According to Eq. (1), the thermal decay depth varies in the range from $0.14/\nu^{0.5}$ to $0.016/\nu^{0.5}$. For the $\nu = 900\ \mathrm{cm}^{-1}$ frequency, the thermal decay length is in the range from 47 to 5 μm. These values are a good prerequisite for the depth profiling of constituents in the 100 μm-thick office-type paper.

The PA spectra of the untreated MB paper and the MB paper laser modified by the procedure described in the previous section are shown in Fig. 6. The 980–750 cm^{-1} spectral range was employed for the analysis due to the better photoacoustic signal to noise ratio as compared to the higher frequency side of the spectrum. The PA signal in this range is a sum of the background formed by the wings of wide 1020 and 650 cm^{-1} bands and two peaks over the background. Peaks at 874 and 898 cm^{-1} belong to $CaCO_3$ [23] and cellulose, respectively. The PA spectra of the hard treated paper are from half to one order of magnitude larger than the PA magnitude for the untreated paper. The spectra magnitude ratio of the treated to untreated paper increases as V increases.

Ten PA spectra of the untreated paper and ten spectra of the laser modified paper were recorded as OPD velocity was varied in ten steps covering the 0.01581 to 1.27 cm/s range. For all PA spectra the peak-to-background magnitude ratio was determined by fitting the measured spectra with composite function. The ratio was taken for the PA signal normalization usual in the praxis of analytical spectroscopy. The least squares fitting was carried out in the 930–830 cm^{-1} interval by the function implying two Gaussian peaks and sloped line representing the background. The sloped line value at the 890 cm^{-1} frequency served as a background magnitude value. Peak heights were output parameters of the least squares fit.

Deconvolution of the PA signal to peaks and background has been carried out to detect the saturation effect mentioned in the previous section. For the saturation detection, the 898 cm^{-1} peak of cellulose matrix was chosen as an indicator. The peak-to-background ratio obtained for the untreated paper shows the increase from 0.2 to 0.45 as V increases from 0.01581 to 0.3 cm/s (Fig. 7). A decrease of the peak-to-background ratio as the OPD velocity decreases indicates onset of the saturation effect. Plateau is observed for V values exceeding 0.3 cm/s. Constancy of the ratio in the plateau range indicates that saturation is insignificant for $V > 0.3$ cm/s. Contrary to the untreated paper the laser-modified paper does not show any significant dependence of the peak-to-background ratio on the OPD velocity (Fig. 7). Independence of normalized PA signal of the scan speed shows the relative resistance of the laser treated sample to the PA signal saturation effect.

For the 874 cm^{-1} $CaCO_3$ peak, the peak-to-background ratio of the laser treated paper is smaller than the corresponding ratio of the untreated paper. This is valid for the entire OPD velocity range. The PA signal decrease following the hard treatment evidently indicates the same as the decrease of the 1793 cm^{-1} $CaCO_3$ peak in the reflectance and transmittance difference spectra does, that is, the amount of $CaCO_3$ in the paper decreases after laser treatment.

4. Conclusions

In summary, the laser energy density cleaning threshold with the 1064 nm subnanosecond laser pulse is almost by an order smaller than the cleaning threshold with the ordinary nanosecond duration laser pulses. Soft laser cleaning of the artificially contaminated paper recovers more than 80% of initial brightness and does not cause noticeable chemical modifications of the paper. The case of laser operating above the paper modification threshold led to the uplifting of the paper surface and thinning-out of cellulose fibres. Thinning of fibres is accompanied by the decrease of $CaCO_3$ 2514, 1793, and 874 cm^{-1} infrared peaks after hard laser treatment. Evidently, the amount of $CaCO_3$ in the paper decreases after laser treatment, but the radiation transfer features in the modified paper cannot be fully excluded as the reason for the calcium carbonate spectral peak decrease. The band absorption variations in the 1627–1650 cm^{-1} range can be explained by the variation of the adsorbed water content.

Photoacoustic FTIR spectroscopy assumes depth profiling in the paper analysis. The hard treated paper generates the 3- to 10-fold larger PA signal as compared to the untreated paper. The normalized PA signal of the 898 cm^{-1} cellulose peak revealed another advantage of laser treatment, that is, the substantial sample resistance to saturation of the photoacoustic signal.

Acknowledgement

This work has been partially supported by the Agency for International Science and Technology Development Programms in Lithuania within the framework of the EUREKA project E!3483 – EULASNET LASCAN.

References

[1] M. Alava and K. Niskanen, The physics of paper, Rep. Prog. Phys. **69**, 669–723 (2006).

[2] W. Kautek, S. Pentzien, P. Rudolph, J. Krüger, and E. König, Laser interaction with coated collagen and cellulose fibre composites: Fundamentals of laser cleaning of ancient parchment manuscripts and paper, Appl. Surf. Sci. **127–129**, 746–754 (1998).

[3] J. Kolar, M. Strlič, S. Pentzien, and W. Kautek, Near-UV, visible and IR pulsed laser light interaction with cellulose, Appl. Phys. A **71**, 87–90 (2000).

[4] J. Kolar, M. Strlič, and M. Marinček, IR pulsed laser light interaction with soiled cellulose and paper, Appl. Phys. A **75**, 673–676 (2002).

[5] K. Ochocińska, A. Kamińska, and G. Śliwiński, Experimantal investigation of stained paper documents cleaned by the Nd : YAG laser pulses, J. Cult. Heritage **4**, 188s–193s (2003).

[6] C. Pérez, M. Barrera, and L. Díez, Positive findings for laser use in cleaning cellulosic supports, J. Cult. Heritage **4**, 194s–200s (2003).

[7] P. Rudolph, F.J. Pedersoli JR, H. Scholten, D. Schipper, J.B.G.A. Havermans, H.A. Aziz, V. Quillet, M. Kraan, B. Van Beek, S. Corr, H.-Y. Hua-Ströfer, J. Stokman, P. Van Dalen, and W. Kautek, Laser-induced alteration of contaminated papers, Appl. Phys. A **79**, 941–944 (2004).

[8] M. Strlič, V.S. Šelf, J. Kolar, D. Kočar, B. Pihlar, R. Ostrowski, J. Marczak, M. Strzelec, M. Marinček, T. Vuorinen, and L.S. Johansson, Optimization and online acoustic monitoring of laser cleaning of soiled paper, Appl. Phys. A **81**, 943–951 (2005).

[9] *Lasers in the Conservation of Artworks. LACONA V Proceedings, Osnabruck, Germany, September 15–18, 2003*, eds: K. Dickmann, C. Fotakis, and J.F. Asmus (Springer-Verlag, Berlin–Heidelberg, 2005).

[10] P. Pregowski, J. Marczak, and A. Koss, Thermal effects on artwork surfaces cleaned with laser ablation method, Proc. SPIE **5146**, 226–235 (2003).

[11] A. Koss and J. Marczak, *Application of Lasers in Conservation of Monuments and Works of Art* (Warsaw, 2005).

[12] M. Bicchieri, S. Ronconi, F.P. Romano, L. Pappalardo, M. Corsi, G. Cristoforetti, S. Legnaioli, V. Palleschi, A. Salvetti, and E. Tognoni, Study of foxing stains on paper by chemical methods, infrared spectroscopy, micro-X-ray fluorescence spectrometry and laser induced breakdown spectroscopy, Spectrochim. Acta B **57**, 1235–1249 (2002).

[13] G. Bitossi, R. Giorgi, M. Mauro, B. Salvadori, and L. Dei, Spectroscopic techniques in cultural heritage conservation: A survey, Appl. Spectrosc. Rev. **40**, 187–228 (2005).

[14] J.F. McClelland, R.W. Jones, and S.J. Bajic, in: *Handbook of Vibrational Spectroscopy*, vol. 2, eds. J.M. Chalmers and P.R. Griffiths (John Wiley & Sons, Chichester, 2002) pp. 1231–1251.

[15] K.H. Michaelian, *Photoacoustic Infrared Spectroscopy* (John Wiley & Sons, New Jersey, 2003).

[16] J. Łojewska, P. Miśkowiec, T. Łojewski, and L.M. Proniewicz, Cellulose oxidative and hydrolytic degradation: In situ FTIR approach, Polymer Degr. Stab. **88**, 512–520 (2005).

[17] J. Łojewska, A. Lubańska, P. Miśkowiec, T. Łojewski, and L.M. Proniewicz, FTIR in situ transmission studies on the kinetic of paper degradation via hydrolytic and oxidative reaction paths, Appl. Phys. A **83**, 597–603 (2006).

[18] L. Jacinavičius, A. Michailovas, and E. Murauskas, Generator of short laser pulses, Patent of Republic of Lithuania, LT 5168 B (2004) [in Lithuanian].

[19] A. Dement'ev, R. Buzelis, E. Kosenko, E. Murauskas, and R. Navakas, Solid-state lasers with pulse compression by transient stimulated Brillouin and Raman scattering, Proc. SPIE **4415**, 92–97 (2001).

[20] A.C. Tam, Applications of photoacoustic sensing techniques, Rev. Mod. Phys. **58**, 381–427 (1986).

[21] E. Martin, The role of thermal properties in periodic time-varying phenomena, Eur. J. Phys. **28**, 429–445 (2007).

[22] J. Coates, in: *Encyclopedia of Analytical Chemistry*, ed. R.A. Meyers (John Wiley & Sons Ltd, Chichester, 2000) pp. 10815–10837.

[23] NIST Chemistry WebBook. Calcium carbonate (precipitated). `webbook.nist.gov/chemistry/` .

[24] J.M. Olinger, P.R. Griffiths, and T. Burger, in: *Handbook of Near-Infrared Analysis*, eds. D.A. Burns and E.W. Ciurczak (Marcel Dekker, New York, 2001) pp. 19–51.

[25] P. Geladi, D. MacDougall, and H. Martens, Linearization and scatter-correction for near-infrared reflectance spectra of meat, Appl. Spectrosc. **39**, 491–500 (1985).

[26] T. Isaksson and T. Naes, The effect of multiplicative scatter correction (MSC) and linearity improvement in NIR spectroscopy, Appl. Spectrosc. **42**, 1273–84 (1988).

UŽTERŠTO POPIERIAUS VALYMAS SUBNANOSEKUNDINIAIS Nd : YAG LAZERIO IMPULSAIS

V. Švedas, A.S. Dementjev, E. Murauskas, N. Slavinskis
Fizikos institutas, Vilnius, Lietuva

Santrauka

Tirtas anglies milteliais užteršto rašomojo popieriaus valymas aktyvios kokybės moduliacijos Nd : YAG lazeriu su priverstinės Brijueno sklaidos impulsų spūda (0,15 ns impulso trukmė ir >10 mJ energija). Valant popierių nefokusuota spinduliuote (impulso energijos tankis $\sim$0,1 J/cm^2), valymo būdas yra švelnus. Šiuo būdu nuvaloma anglis ir lazerio spinduliuote atstatoma daugiau nei 80% popieriaus pirminio baltumo. Švelnų valymą lydintys cheminiai popieriaus pokyčiai yra žemiau FTIR spektroskopijos aptikimo ribos. Veikiant popierių fokusuota spinduliuote (impulso energijos tankis $\sim$5 J/cm^2), gaunamas stiprus poveikis, kuris sukelia popieriaus paviršiaus pakilimą ir celiuliozės skaidulų išretėjimą. FTIR pralaidos, atspindžio bei fotoakustiniams matavimams paruošiamas $\sim$1 cm^2 popierius plotas, atliekant kompiuteriu valdomą X–Y skenavimą. Stipraus poveikio sukelti morfologiniai popieriaus pakitimai yra lydimi cheminių pokyčių. Skaidulų išretėjimą lydi $CaCO_3$ spektrinių smailių ties 1793 ir 874 cm^{-1} bei 2514 cm^{-1} juostos intensyvumų sumažėjimas, kurį galima paaiškinti kalcio karbonato koncentracijos sumažėjimu. 1650–1627 cm^{-1} intervalo spektrinių juostų intensyvumų kitimai siejami su popieriuje adsorbuoto vandens kiekiu.

Fotoakustinė spektroskopija leidžia atlikti cheminės sudėties spektrinę analizę, įskaitant pasiskirstymą bandinio gylyje. Stipraus lazerio poveikio sukelti sandaros pokyčiai suteikia popieriui savybių, palankių fotoakustinei spektroskopijai – signalas padidėja nuo 3 iki 10 kartų, pagerėja modifikuoto popieriaus atsparumas fotoakustinio signalo įsisotinimo reiškiniui.